

B-meson dileptonic decays enhanced by supersymmetry with large $\tan\beta$

Zhaohua Xiong ^{a,b,c} and Jin Min Yang ^b

^a CCAST (World Laboratory), P.O.Box 8730, Beijing 100080, China

^b Institute of Theoretical Physics, Academia Sinica, Beijing 100080, China

^c Institute of High Energy Physics, Academia Sinica, Beijing 100039, China

(October 29, 2018)

We examined the rare decays $B \rightarrow X_s \ell^+ \ell^-$ and $B_s \rightarrow \ell^+ \ell^- \gamma$ in the minimal supersymmetric model with large $\tan\beta$. Taking into account the gluino-loop and neutralino-loop effects, we found that for a large $\tan\beta$ the neutral Higgs exchanging diagrams could enhance $Br(B \rightarrow X_s \tau^+ \tau^-)$ by a factor of 5 and $Br(B_s \rightarrow \tau^+ \tau^- \gamma)$ by a couple of orders in some part of supersymmetric parameter space allowed by current experiments such as $b \rightarrow s\gamma$, $B \rightarrow K^{(*)} \ell^+ \ell^-$ and $B_s \rightarrow \ell^+ \ell^-$. The forward-backward asymmetry and the distributions of differential branching ratios are also found to differ significantly from the standard model results. Such enhanced branching ratios reach the level of 10^{-5} and thus might be observable in the new generation of B experiments.

12.15.Mm, 12.60.Fr, 12.60.Jv, 13.25.Hw

I. INTRODUCTION

Flavor-changing neutral-currents (FCNC) induced B-meson rare decays provide an ideal opportunity for extracting information about the fundamental parameters of the standard model (SM), testing the SM predictions at loop level and probing possible new physics. After the observation of the penguin-induced decay $B \rightarrow X_s \gamma$ and the corresponding exclusive channels such as $B \rightarrow K^* \gamma$ [1], rare B-decays have begun to play an important role in the phenomenology of particle physics. The latest measured decay ratio for $B \rightarrow X_s \gamma$ by CLEO and BELLE [2] is in good agreement with the SM prediction, putting strong constraints on its various extensions and therefore stimulating the study of radiative rare B-meson decays with a new momentum.

Among rare B-meson decays, $B_s \rightarrow \ell^+ \ell^- \gamma$ ($\ell = e, \mu, \tau$) are of special interest due to their relative cleanliness and sensitivity to models beyond the SM [3–5]. Since in these processes a photon is emitted in addition to the lepton pair, no helicity suppression exists and “large” branching ratio is expected. Other interesting decay modes in this context are the inclusive transitions $B \rightarrow X_s \ell^+ \ell^-$. Although these rare decays have not been observed, their detection is expected at the B-factories which are currently running.

These decays have been studied in the SM [6] and recently, to reduce the theoretical uncertainties, the next-to-next-to leading order(NNLO) corrections were completed [7]. New physics effects in these decays have also been studied in some models, such as the minimal supersymmetric model (MSSM) [8–11], the two Higgs doublet model(2HDM) [12–15] and the technicolor model [5].

It is noticeable that in the SM the matrix elements of $B \rightarrow X_s \ell^+ \ell^-$ and $B_s \rightarrow \ell^+ \ell^- \gamma$ are strongly suppressed by a factor m_ℓ/m_W and the contributions from exchanging neutral Higgs boson can be safely neglected. In the MSSM [16], the situation is different, specially in the case of $\ell = \tau$ with large $\tan\beta$. In this model, as studied in [11], the contributions from exchanging neutral Higgs bosons are enhanced roughly by a factor $\tan^3\beta$ and may no longer be negligible since currently a large $\tan\beta$ is favored both by LEP experiments [17] and by the supersymmetry (SUSY) explanation [18] of the measurement for the muon anomalous magnetic moment [19].

We note that the most previous studies on the contributions from exchanging neutral Higgs bosons [9–11] mainly focused on the charged-current loop effects; the effects of neutral-current loops (NCL), such as gluino-loop and neutralino-loop, have been considered only for $B_{d,s}^0 \rightarrow \mu^+ \mu^-$ using mass insert approximation method in [8]. A detail general calculation for such NCL effects is necessary. The NCL can be induced via the flavor mixing of down-type squarks and might be important for the following reasons. Firstly, such flavor mixings of sfermions are almost unavoidable in supersymmetric models. In fact, in the framework of MSSM sfermions may have arbitrary flavor mixings in the soft breaking terms; while in some constrained MSSM, such as low-energy supergravity models, the flavor mixings at weak scale could be naturally generated through renormalization equation even the flavor diagonality is assumed at the Planck scale [20]. Secondly, the flavor mixings between the third and the second generation squarks are subject to no strong low-energy constraints like $K^0 - \bar{K}^0$ mixing. Thirdly, the large $\tan\beta$ will give rise to large mass splitting between two mass eigenstates of sbottoms, making the lighter sbottom (b_1) even lighter.

In this article, we will present a complete calculation of MSSM effects in the decays $B_s \rightarrow \ell^+ \ell^- \gamma$ and $B \rightarrow X_s \ell^+ \ell^-$ ($\ell = e, \mu, \tau$), taking into account the contributions from the neutral Higgs exchange with NCL. We will evaluate

the effects on branching ratios, the forward-backward asymmetry as well as the distributions of differential branching ratios. In Section II, we will give a brief description of the squark mixing in the MSSM. The detailed calculations for Wilson coefficients of scalar and pseudo-scalar operators are included in Section III. The decays $B \rightarrow X_s \ell^+ \ell^-$ and $B_s \rightarrow \ell^+ \ell^- \gamma$ are calculated in Section IV. Experimental constraints on the parameter space of the MSSM are discussed in Section V. Some numerical results are presented in Section VI. Finally, in Section VII, we give our conclusion.

II. SQUARK MIXINGS IN MSSM

The squark mass terms arise from the scalar potential which contains the supersymmetric F-term and D-term as well as the soft SUSY breaking terms. These soft breaking terms may have arbitrary flavor mixings. As a result, the squark mass terms in flavor basis, i.e., $\tilde{U} = (\tilde{u}_L, \tilde{c}_L, \tilde{t}_L, \tilde{u}_R, \tilde{c}_R, \tilde{t}_R)$ and $\tilde{D} = (\tilde{d}_L, \tilde{s}_L, \tilde{b}_L, \tilde{d}_R, \tilde{s}_R, \tilde{b}_R)$, take the forms

$$\tilde{M}_{\tilde{U}}^2 = \begin{bmatrix} M_{\tilde{Q}}^2 + m_{\tilde{U}}^2 + m_Z^2(\frac{1}{2} - e_U \sin^2 \theta_W) \cos 2\beta & m_U(A_u - \mu \cot \beta) \\ m_U(A_u - \mu \cot \beta) & M_{\tilde{U}}^2 + m_{\tilde{U}}^2 + m_Z^2 e_U \sin^2 \theta_W \cos 2\beta \end{bmatrix}, \quad (2.1)$$

$$\tilde{M}_{\tilde{D}}^2 = \begin{bmatrix} M_{\tilde{Q}}^2 + m_{\tilde{D}}^2 - m_Z^2(\frac{1}{2} + e_D \sin^2 \theta_W) \cos 2\beta & m_D(A_u - \mu \tan \beta) \\ m_D(A_u - \mu \tan \beta) & M_{\tilde{D}}^2 + m_{\tilde{D}}^2 + m_Z^2 e_D \sin^2 \theta_W \cos 2\beta \end{bmatrix}, \quad (2.2)$$

where $e_U = 2/3$, $e_D = -1/3$, $m_{U(D)}$ is the 3×3 diagonal mass matrix for up(down)-type quarks. $M_{\tilde{Q}}^2$, $M_{\tilde{U}}^2$ and $M_{\tilde{D}}^2$ are soft-breaking mass terms for left-handed squark doublet \tilde{Q} , right-handed up and down squarks, respectively. A_u (A_d) is the coefficient of the trilinear term $H_2 \tilde{Q} \tilde{U}$ ($H_1 \tilde{Q} \tilde{D}$) in soft-breaking terms and $\tan \beta = v_2/v_1$ is ratio of the vacuum expectation values of the two Higgs doublets. The hermitian matrices $\tilde{M}_{\tilde{U},\tilde{D}}^2$ can be diagonalized by the unitary relations, which transfer the interaction eigenstates into the physical mass eigenstates. So in the general MSSM, without knowing the mechanism of SUSY breaking, squarks could have arbitrary flavor mixings.

However, the flavor mixings in the first two generations are subject to strong phenomenological constraints, such as $K^0 - \bar{K}^0$ mixing. So we only consider the flavor mixings between the second and third generations, i.e., between \tilde{b} and \tilde{s} . Further, like the analysis in [22], we suppose the tree level Lagrangian is flavor diagonal and the flavor mixing is induced via loops. The dominant effects are from the logarithmic divergences caused by soft breaking terms. Such divergences must be subtracted using a soft counter-term at the SUSY breaking scale, such as Planck scale M_p . Thus a large logarithm factor $\ln(M_p^2/m_W^2) \approx 80$ remains after renormalization. In the approximation of neglecting the strange quark mass, \tilde{s}_R does not mix with sbottoms. The mixing of \tilde{s}_L with sbottoms results in the physical states is given by

$$\begin{pmatrix} \tilde{s}_1 \\ \tilde{b}_1 \\ \tilde{b}_2 \end{pmatrix} = T^D \begin{pmatrix} \tilde{s}_L \\ \tilde{b}_L \\ \tilde{b}_R \end{pmatrix} = \begin{pmatrix} 1 & \epsilon'_1 & \epsilon'_2 \\ \epsilon_1 & \cos \theta_b & \sin \theta_b \\ \epsilon_2 & -\sin \theta_b & \cos \theta_b \end{pmatrix} \begin{pmatrix} \tilde{s}_L \\ \tilde{b}_L \\ \tilde{b}_R \end{pmatrix}, \quad (2.3)$$

where

$$\begin{aligned} \epsilon_1 &= -c_b \frac{m_t^2}{\sin^2 \beta} \left[\frac{(M_{\tilde{Q}}^2 + M_{\tilde{U}}^2 + M_{H_1}^2 + |A_t|^2) \cos \theta_b + m_b A_t^* \sin \theta_b}{m_{\tilde{b}_1}^2 - m_{\tilde{s}_1}^2} \right], \\ \epsilon_2 &= -c_b \frac{m_t^2}{\sin^2 \beta} \left[\frac{-(M_{\tilde{Q}}^2 + M_{\tilde{U}}^2 + M_{H_1}^2 + |A_t|^2) \sin \theta_b + m_b A_t^* \cos \theta_b}{m_{\tilde{b}_2}^2 - m_{\tilde{s}_2}^2} \right], \\ \epsilon'_1 &= -\epsilon_1 \cos \theta_b + \epsilon_2 \sin \theta_b, \\ \epsilon'_2 &= -\epsilon_1 \sin \theta_b - \epsilon_2 \cos \theta_b. \end{aligned} \quad (2.4)$$

Here θ_b is the left-right sbottom mixing angle, K_{ij} are the CKM-matrix elements, and $c_b = \frac{\alpha_{em}}{4\pi} \frac{K_{tb}^* K_{ts}}{2m_W \sin^2 \theta_W} \ln \frac{M_p^2}{m_W^2}$.

Note the mixing matrix T^U between the left-handed scharm and stops takes the similar form as T^D , and under the assumption that the flavor mixing between the second and third generation squarks is at least one order lower than the third left- and right-hand squarks mixing, the rotation matrix $T^{U,D}$ are approximately unitarity.

III. CALCULATION OF SCALAR AND PSEUDO-SCALAR WILSON COEFFICIENTS

In the MSSM, the short distance contribution to $b \rightarrow s\ell^+\ell^-$ decay can be computed in the framework of the QCD corrected effective weak Hamiltonian, obtained by integrating out heavy particles, i.e., top quark, W^\pm , Z bosons in the SM and the sparticles,

$$\mathcal{H}_{eff} = -\frac{4G_F}{\sqrt{2}}K_{tb}K_{ts}^* \sum_{i=1}^{10} [C_i(\mu_r)\mathcal{O}_i(\mu_r) + C_{Q_i}(\mu_r)\mathcal{Q}_i(\mu_r)] , \quad (3.1)$$

where \mathcal{O}_i , \mathcal{Q}_i are operators given in Eqs. (7.1) [12], (7.2) [13] and C_i, C_{Q_i} are Wilson coefficients renormalized at the scale μ_r ¹.

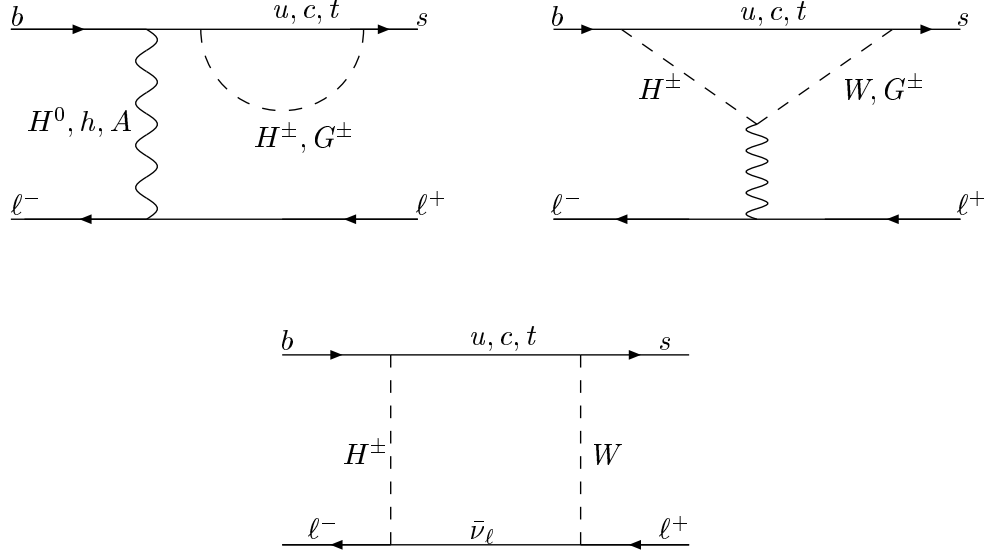


FIG. 1. The Feynman diagrams involving charged Higgs which give dominate contribution to $C_{Q_{1,2}}$

In the MSSM the additional contributions to operators in Eq. (3.1) can be characterized by the values of the coefficients C_i and C_{Q_i} at the perturbative scale m_W . For the processes we will study, it is only relevant with the effective Wilson coefficients $C_{7,9,10}$ which have been computed in Ref. [10] and $C_{Q_{1,2}}$ of additional scalar and pseudo-scalar operators. In this section we will focus our attention on the calculation of the Wilson coefficients $C_{Q_{1,2}}(m_W)$ with the assumption that except for the third generation squarks all sfermions are degenerate and have a mass of ~ 1 TeV. Besides the contribution from box diagrams, the neutral Higgs-bosons exchange diagrams include totally five classes of loops: (1) W boson and up-type quarks, (2) charged Higgs and up-type quarks, (3) charginos and up-type squarks, (4) neutralinos and down-type squarks, and (5) gluinos and down-type squarks. As pointed out in Section I, the last two classes of loops have not been calculated in the literatures. Now we take all of them into account and use the Feynman rules presented in [16]. Since we are only interested in large $\tan\beta$ case, for simplicity we ignore less important terms and keep only the leading part contributions given in the following:

- Charged Higgs (Fig. 1)

$$C_{Q_1}^{H^\pm}(m_W) = -C_{Q_2}^{H^\pm}(m_W) = \frac{m_\ell m_b \tan^2 \beta}{m_W^2} \frac{1}{4} P_1(x_{H^\pm t}) \quad (3.2)$$

¹The most general Hamiltonian in low-energy supersymmetry also contains the operators \mathcal{O}'_i , \mathcal{Q}'_i which are flipped chirality partners of \mathcal{O}_i , \mathcal{Q}_i . However, they give negligible contributions and thus not considered in the final discussion of physical quantities [23].

where $x_{ij} = m_i^2/m_j^2$ and the one-loop integral functions P_i are given in the appendix.

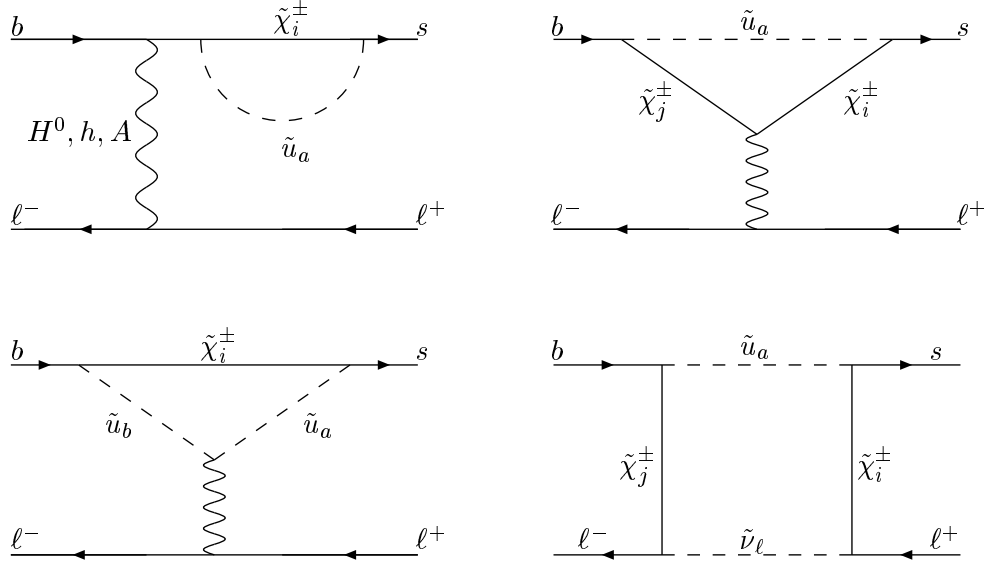


FIG. 2. The Feynman diagrams involving chargino which give dominate contribution to $C_{Q_{1,2}}$

- Chargino (Fig. 2)

$$\begin{aligned}
C_{Q_1}^{\tilde{\chi}^\pm}(m_W) = & -\frac{m_\ell m_b}{4} \tan^2 \beta \sum_{i,i'=1}^2 \sum_{k,k'=1}^3 \Gamma_1(i, k, k') U_{i'2} \left\{ \delta_{ii'} \delta_{kk'} \frac{\sqrt{2}}{\cos \beta} \frac{m_{\tilde{\chi}_i^\pm}}{m_W} r_+ P_1(x_{\tilde{\chi}_i^\pm} \tilde{t}_{k-1}) \right. \\
& - \delta_{kk'} \Gamma_2^*(i', i) r_+ P_2(x_{\tilde{t}_{k-1} \tilde{\chi}_i^\pm}, x_{\tilde{\chi}_{i'}^\pm \tilde{\chi}_i^\pm}) - \delta_{kk'} \frac{m_{\tilde{\chi}_{i'}^\pm}}{m_{\tilde{\chi}_i^\pm}} \Gamma_2(i, i') P_3(x_{\tilde{t}_{k-1} \tilde{\chi}_i^\pm}, x_{\tilde{\chi}_{i'}^\pm \tilde{\chi}_i^\pm}) \\
& + \delta_{ii'} \sqrt{2} \frac{m_W}{m_{\tilde{\chi}_i^\pm}} \left(r_0 \frac{\frac{1}{2} - \frac{2}{3} \sin^2 \theta_W}{\cos^2 \theta_W} - \Gamma_3(k, k') \right) P_3(x_{\tilde{t}_{k-1} \tilde{\chi}_i^\pm}, x_{\tilde{t}_{k'-1} \tilde{\chi}_i^\pm}) \\
& \left. + \delta_{kk'} \frac{m_{\tilde{\chi}_{i'}^\pm}}{m_{\tilde{\chi}_i^\pm}^3} V_{i1} U_{i'2} P_4(x_{\tilde{m} \tilde{\chi}_i^\pm}, x_{\tilde{\chi}_{i'}^\pm \tilde{\chi}_i^\pm}, x_{\tilde{t}_{k-1} \tilde{\chi}_i^\pm}) \right\}, \tag{3.3}
\end{aligned}$$

$$\begin{aligned}
C_{Q_2}^{\tilde{\chi}^\pm}(m_W) = & \frac{m_\ell m_b}{4m_A^2} \tan^2 \beta \sum_{i,i'=1}^2 \sum_{k,k'=1}^3 \Gamma_1(i, k, k') U_{i'2} \left\{ \delta_{ii'} \delta_{kk'} \frac{\sqrt{2}}{\cos \beta} \frac{m_{\tilde{\chi}_i^\pm}}{m_W} P_1(x_{\tilde{\chi}_i^\pm} \tilde{t}_{k-1}) \right. \\
& - 2\delta_{kk'} V_{i'1} U_{i2} P_2(x_{\tilde{t}_{k-1} \tilde{\chi}_i^\pm}, x_{\tilde{\chi}_{i'}^\pm \tilde{\chi}_i^\pm}) + 2\delta_{kk'} V_{i1} U_{i'2} \frac{m_{\tilde{\chi}_{i'}^\pm}}{m_{\tilde{\chi}_i^\pm}} P_3(x_{\tilde{t}_{k-1} \tilde{\chi}_i^\pm}, x_{\tilde{\chi}_{i'}^\pm \tilde{\chi}_i^\pm}) \\
& + \delta_{ii'} \sqrt{2} \frac{m_t}{m_W} \frac{\mu}{m_{\tilde{\chi}_i^\pm}} (T_{k2}^U T_{k'3}^U - T_{k3}^U T_{k'2}^U) P_3(x_{\tilde{t}_{k-1} \tilde{\chi}_i^\pm}, x_{\tilde{t}_{k'-1} \tilde{\chi}_i^\pm}) \\
& \left. - \delta_{kk'} x_{A \tilde{\chi}_i^\pm} \frac{m_{\tilde{\chi}_{i'}^\pm}}{m_{\tilde{\chi}_i^\pm}} V_{i1} U_{i'2} P_4(x_{\tilde{m} \tilde{\chi}_i^\pm}, x_{\tilde{\chi}_{i'}^\pm \tilde{\chi}_i^\pm}, x_{\tilde{t}_{k-1} \tilde{\chi}_i^\pm}) \right\}, \tag{3.4}
\end{aligned}$$

where α is the mixing angle of neutral components of the two Higgs doublets, $r_+ = \cos^2 \alpha m_H^{-2} + \sin^2 \alpha m_h^{-2}$, $r_0 = \sin 2\alpha (m_H^{-2} - m_h^{-2})$, $\lambda_t = m_t / \sqrt{2} m_W \sin \beta$ and $\lambda_b = m_b / \sqrt{2} m_W \cos \beta$ are the Yukawa couplings of top and bottom quarks, respectively. U , V and N are the matrices which diagonalise the chargino and neutralino mass matrices. $\tilde{m} = m_{\tilde{t}_0} = m_{\tilde{b}_0}$ is defined as the common mass of the first two generation squarks and all sleptons which are assumed to be degenerate, $N'_j = \frac{1}{3} \tan \theta_W N_{j1} - N_{j2}$, and

$$\begin{aligned}
\Gamma_1(i, k, k') &= \begin{cases} -V_{i1} \left(\frac{K_{cs}^*}{K_{ts}^*} T_{12}^U - 1 \right) & \text{for } k, k' = 1 \\ \left[-V_{i1} \left(T_{k1}^U \frac{K_{cs}^*}{K_{ts}^*} + T_{k2}^U \right) + \lambda_t V_{i2} T_{k3}^U \right] T_{k'2}^U, \end{cases} \\
\Gamma_2(i, i') &= 2r_+ V_{i1} U_{i'2} + r_0 V_{i2} U_{i'1}, \\
\Gamma_3(k, k') &= \frac{m_t (r_0 A_t + 2r_0 m_t + 2r_+ \mu)}{2m_W^2} (T_{k2}^U T_{k'3}^U + T_{k3}^U T_{k'2}^U) - r_0 \frac{2}{3} \tan^2 \theta_W T_{k3}^U T_{k'3}^U, \\
\Gamma_4(j, k) &= \frac{2}{3} \tan \theta_W N_{j1} T_{k3}^D + \sqrt{2} \lambda_b N_{j3}^* T_{k2}^D, \\
\Gamma_5(j, j', j'') &= \frac{1}{2} N_{j'3} [N_{jj''} (N_{j'2} - N_{j'1} \tan \theta_W) + N_{j'j''} (N_{j2} - N_{j1} \tan \theta_W)], \\
\Gamma_6(k, k', j) &= r_0 N_{j3} * T_{k'2}^D \left(\frac{\frac{1}{2} - \frac{1}{3} \sin^2 \theta_W}{\cos^2 \theta_W} - \frac{1}{3} \tan^2 \theta_W T_{k3}^D T_{k'3}^D \right) \\
&\quad + \frac{r_0 \mu + 2r_+ A_b}{3m_W} \tan \theta_W T_{k'3}^D (T_{k2}^D T_{k'3}^D + T_{k3}^D T_{k'2}^D), \\
\Gamma_7(k, j, j') &= [N_{j3} (N_{j'2} + \tan \theta_W N_{j'1}) - 2 \tan \theta_W N_{j1} N_{j'3}] N_{j'3} T_{k2}^D, \\
\Gamma_8(k, j, j') &= 2 \tan \theta_W (N_{j3}^* (N_{j'1} - N_{j1} N_{j'3}) N_{j3} T_{k3}^D). \tag{3.5}
\end{aligned}$$

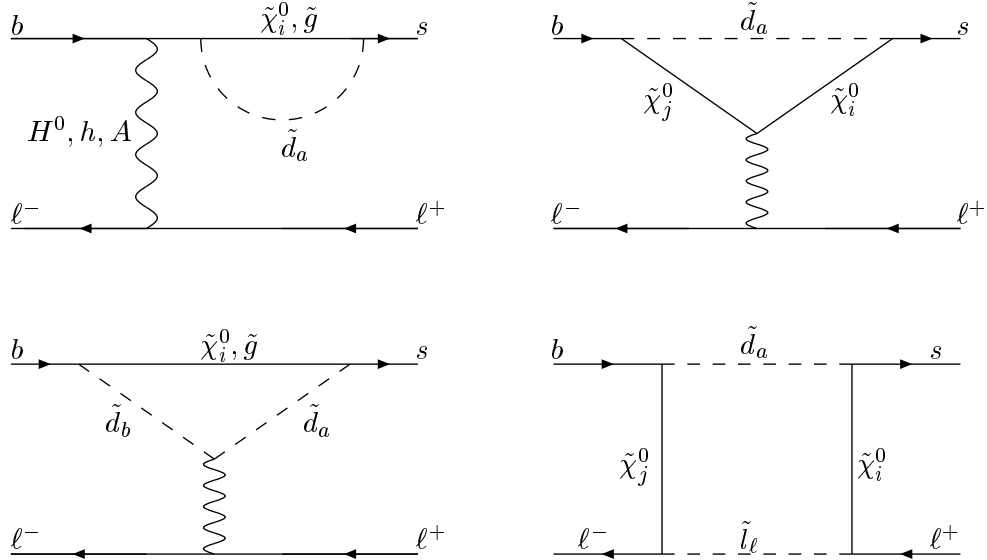


FIG. 3. The Feynman diagrams involving neutralino which give dominate contribution to $C_{Q_{1,2}}$

- Neutralino (Fig. 3)

The formula for the contribution from the neutralino are given by

$$\begin{aligned}
C_{Q_1}^{\tilde{\chi}_1^0}(m_W) &= \frac{m_\ell m_b}{4} \frac{1}{K_{ts}^* K_{tb}} \tan^2 \beta \sum_{j,j'=1}^4 \sum_{k,k'=1}^3 N_j^* T_{k1}^D \left\{ \delta_{jj'} \delta_{kk'} \frac{m_{\tilde{\chi}_j^0}}{m_b} \Gamma_4(j, k) r_+ P_1 \left(x_{\tilde{\chi}_j^0 \tilde{b}_{k-1}} \right) \right. \\
&\quad + \delta_{kk'} (2r_+ \Gamma_5^*(j', j, 3) - r_0 \Gamma_5^*(j', j, 4)) T_{k2}^D P_2 \left(x_{\tilde{\chi}_j^0 \tilde{b}_{k-1}}, x_{\tilde{\chi}_{j'}^0 \tilde{b}_{k-1}} \right) \\
&\quad + \delta_{kk'} \frac{m_{\tilde{\chi}_{j'}^0}}{m_{\tilde{\chi}_j^0}} (2r_+ \Gamma_5(j, j', 3) - r_0 \Gamma_5(j, j', 4)) T_{k2}^D P_3 \left(x_{\tilde{b}_{k-1} \tilde{\chi}_j^0} x_{\tilde{\chi}_{j'}^0 \tilde{\chi}_j^0} \right) \\
&\quad \left. - \delta_{jj'} \frac{m_W}{m_{\tilde{\chi}_j^0}} \Gamma_6(k, k', j) P_3 \left(x_{\tilde{b}_{k-1} \tilde{\chi}_j^0}, x_{\tilde{b}_{k'-1} \tilde{\chi}_j^0} \right) \right\}
\end{aligned}$$

$$-\delta_{kk'} \frac{1}{2} \frac{m_{\tilde{\chi}_{j'}}^0}{m_{\tilde{\chi}_j^0}^3} (\Gamma_7(k, j, j') + \Gamma_8(k, j, j')) P_4 \left(x_{\tilde{m}\tilde{\chi}_j^0}, x_{\tilde{\chi}_{j'}^0}, \tilde{\chi}_j^0 x_{\tilde{b}_{k-1}\tilde{\chi}_j^0} \right) \Big\}, \quad (3.6)$$

$$\begin{aligned} C_{Q_2}^{\tilde{\chi}_j^0}(m_W) = & -\frac{m_\ell m_b}{4m_A^2} \frac{1}{K_{ts}^* K_{tb}} \tan^2 \beta \sum_{j,j'=1}^4 \sum_{k,k'=1}^3 N_j' T_{k1}^D \left\{ \delta_{jj'} \delta_{kk'} \frac{m_{\tilde{\chi}_j^0}}{m_b} \Gamma_4(j, k) P_1 \left(x_{\tilde{\chi}_j^0 \tilde{b}_{k-1}} \right) \right. \\ & - 2\delta_{kk'} \Gamma_5^*(j', j, 3) T_{k2}^D P_2 \left(x_{\tilde{\chi}_j^0 \tilde{b}_{k-1}}, x_{\tilde{\chi}_{j'}^0, \tilde{b}_{k-1}} \right) + 2\delta_{kk'} \frac{m_{\tilde{\chi}_{j'}}^0}{m_{\tilde{\chi}_j^0}} \Gamma_5(j, j', 3) T_{k2}^D P_3 \left(x_{\tilde{b}_{k-1}\tilde{\chi}_j^0}, x_{\tilde{\chi}_{j'}^0}, \tilde{\chi}_j^0 \right) \\ & - \delta_{jj'} \left(\frac{\mu}{m_{\tilde{\chi}_j^0}} T_{k'2}^D - \frac{2A_b}{3m_{\tilde{\chi}_j^0}} \tan \theta_W T_{k'3}^D \right) N_{j1} P_3 \left(x_{\tilde{b}_{k-1}\tilde{\chi}_j^0}, x_{\tilde{b}_{k'-1}\tilde{\chi}_j^0} \right) \\ & \left. + \delta_{kk'} \frac{1}{2} x_{A\tilde{\chi}_j^0} \frac{m_{\tilde{\chi}_{j'}}^0}{m_{\tilde{\chi}_j^0}} (\Gamma_7(k, j, j') - \Gamma_8(k, j', j)) P_4 \left(x_{\tilde{m}\tilde{\chi}_j^0}, x_{\tilde{\chi}_j^0}, \tilde{\chi}_j^0 x_{\tilde{b}_{k-1}\tilde{\chi}_j^0} \right) \right\}. \quad (3.7) \end{aligned}$$

- Gluino (Fig. 3)

$$\begin{aligned} C_{Q_1}^{\tilde{g}}(m_W) = & -\frac{m_\ell m_b}{4} \frac{16g_s^2}{3g^2 K_{ts}^* K_{tb}} \tan^2 \beta \sum_{k,k'=1}^3 T_{k1}^D T_{k'3}^D \left[\delta_{kk'} r_+ \frac{m_{\tilde{g}}}{m_b} P_1(x_{\tilde{g}\tilde{b}_{k-1}}) \right. \\ & \left. + \frac{r_0\mu + 2r_+ A_b}{2m_{\tilde{g}}} (T_{k2}^D T_{k'3}^D + T_{k3}^D T_{k'2}^D) P_3(x_{\tilde{b}_{k-1}\tilde{g}}, x_{\tilde{b}_{k'-1}\tilde{g}}) \right], \\ C_{Q_2}^{\tilde{g}}(m_W) = & \frac{m_\ell m_b}{4m_A^2} \frac{16g_s^2}{3g^2 K_{ts}^* K_{tb}} \tan^2 \beta \sum_{k,k'=1}^3 T_{k1}^D T_{k'3}^D \left[\delta_{kk'} \frac{m_{\tilde{g}}}{m_b} P_1(x_{\tilde{g}\tilde{b}_{k-1}}) \right. \\ & \left. + \frac{A_b}{m_{\tilde{g}}} (T_{k2}^D T_{k'3}^D - T_{k3}^D T_{k'2}^D) P_3(x_{\tilde{b}_{k-1}\tilde{g}}, x_{\tilde{b}_{k'-1}\tilde{g}}) \right]. \quad (3.8) \end{aligned}$$

It is noticeable that the supersymmetric contributions to $C_{Q_{1,2}}$ have an overall enhancement factor $\tan^2 \beta$. Moreover, the gluino loop contributions have an additional enhancement factor $\frac{16g_s^2}{3g^2 K_{ts}^* K_{tb}} \frac{m_{\tilde{g}}}{m_b}$. So sizable contributions from neutral Higgs penguin diagrams are expected for a sufficiently large $\tan \beta$.

IV. B RARE DILEPTONIC DECAYS IN THE MSSM

A. Inclusive decay $B \rightarrow X_s \ell^+ \ell^-$

Neglecting the strange quark mass, and with p standing for the momentum transfer, the effective Hamiltonian (3.1) leads to the following matrix element for the inclusive $b \rightarrow s \ell^+ \ell^-$ decay,

$$\begin{aligned} \mathcal{M} = & \frac{\alpha_{em} G_F}{2\sqrt{2}\pi} K_{tb} K_{ts}^* \left\{ -2C_7^{eff} \frac{m_b}{p^2} \bar{s} i \sigma_{\mu\nu} p_\nu (1 + \gamma_5) b \right. \\ & + C_9^{eff} \bar{s} \gamma_\mu (1 - \gamma_5) b \bar{\ell} \gamma_\mu \ell + C_{10} \bar{s} \gamma_\mu (1 - \gamma_5) b \bar{\ell} \gamma_\mu \gamma_5 \ell \\ & \left. + C_{Q_1} \bar{s} (1 + \gamma_5) b \bar{\ell} \ell + C_{Q_2} \bar{s} (1 + \gamma_5) b \bar{\ell} \gamma_5 \ell \right\}. \quad (4.1) \end{aligned}$$

The Wilson coefficients can be evaluated from m_W down to the lower scale of about m_b by using the renormalization group equation. When evolving down to b quark scale, the operators \mathcal{O}_j ($j = 1 - 6$), Q_3 can mix with \mathcal{O}_i , ($i = 7, 9$); however, they can be included in an “effective” $\mathcal{O}_{7,9}$ because of their same structures contributing to the $b \rightarrow s \ell^+ \ell^-$ matrix element. As for long-distance contribution from the intermediate J/Ψ family, we follow Ref. [25] and include the effect in “effective” C_9^{eff} . Expanding C_i in powers of α_s , i.e., $C = C^0 + \frac{\alpha_s}{4\pi} C^1$, one obtains the leading order effective Wilson coefficients [12–14]

$$C_7^{0,eff}(m_b) = \eta^{16/23} \left[C_7^{0,eff}(m_W) + \frac{8}{3} (\eta^{-2/23} - 1) C_8^{0,eff}(m_W) - 0.012 C_{Q_3}(m_W) \right] + \sum_{i=1}^8 h_i \eta^{a_i}, \quad (4.2)$$

$$\begin{aligned}
C_9^{0,eff}(m_b) &= C_9^{0,eff}(m_W) + \frac{2}{9} [3C_3 + C_4 + 3C_5 + C_6] \\
&\quad - \frac{1}{2}g(1, s) [4C_3 + 4C_4 + 3C_5 + C_6] - \frac{1}{2}g(0, s) [C_3 + 3C_4] \\
&\quad + \left\{ g\left(\frac{m_c^2}{m_b^2}, s\right) - \frac{3\pi}{\alpha_{em}^2} \kappa \sum_{V_i=\Psi', \Psi'', \dots} \frac{m_{V_i} \Gamma(V_i \rightarrow \ell^+ \ell^-)}{m_{V_i}^2 - p^2 - im_{V_i} \Gamma_{V_i}} \right\} \\
&\quad \times [3C_1 + C_2 + 3C_3 + C_4 + 3C_5 + C_6], \tag{4.3}
\end{aligned}$$

$$C_{10}^0(m_b) = C_{10}(m_W), \tag{4.4}$$

$$C_{Q_i}(m_b) = \eta^{-12/23} C_{Q_i}(m_W). \tag{4.5}$$

Here $s = p^2/m_b^2$ is the scaled dilepton invariant mass square, $\eta = \alpha_s(m_W)/\alpha_s(m_b)$, vector h_i, a_i, f_i and g_i are given in [24] and

$$C_{Q_3}(m_W) = \frac{m_b}{m_\tau} (C_{Q_1}(m_W) + C_{Q_2}(m_W)), \tag{4.6}$$

$$C_{1-6} = (-0.4561, 1.0208, -0.0041, -0.0603, 0.0028, 0.0037). \tag{4.7}$$

At NLO level, the Wilson coefficient $C_4^{1,eff}$ can be found in [24] and

$$\begin{aligned}
C_7^{1,eff}(m_b) &= \frac{37208}{4761} \eta^{16/23} (\eta - 1) C_7^{0,eff}(m_W) + \eta^{39/23} C_7^{1,eff}(m_W) + \frac{8}{3} \eta^{37/23} (1 - \eta^{2/23}) C_8^{1,eff}(m_W) \\
&\quad + \frac{4}{14283} \eta^{14/23} \left[64217\eta + 74416\eta^{2/23} - \frac{1791104}{25} - \frac{1674721}{25} \eta^{25/23} \right] C_8^{0,eff} \\
&\quad + \sum_{i=1}^8 \left[e_i \eta C_4^{1,eff}(m_W) + f_i + g_i \eta \right] \eta^{a_i}, \tag{4.8}
\end{aligned}$$

$$\begin{aligned}
C_9^{1,eff}(m_b) &= \frac{1}{12} C_9^{0,eff}(m_W) \left[-4Li_2(s) - 2\ln(s) \ln(1-s) - \frac{2}{3}\pi^2 - \frac{5+4s}{1+2s} \ln(1-s) \right. \\
&\quad \left. - \frac{2s(1+s)(1-2s)}{(1-s)^2(1+2s)} \ln(s) + \frac{5+9s-6s^2}{2(1-s)(1+2s)} \right]. \tag{4.9}
\end{aligned}$$

Function $g(m_c^2/m_b^2, s)$ in Eq. (4.3) arises from the one-loop matrix elements of the four-quark operators, and

$$g(x, y) = -\frac{4}{9} \ln x + \frac{8}{27} + \frac{16x}{9y} - \frac{4}{9} \left(1 + \frac{2x}{y}\right) \left|1 - \frac{4x}{y}\right|^{1/2} \begin{cases} \ln Z(x, y) - i\pi & \text{for } 4x/y < 1 \\ 2 \arctan \frac{1}{\sqrt{4x/y-1}} & \text{for } 4x/y > 1 \end{cases} \tag{4.10}$$

where

$$Z(x, y) = \frac{1 + \sqrt{1 - \frac{4x}{y}}}{1 - \sqrt{1 - \frac{4x}{y}}}. \tag{4.11}$$

To estimate the long-distance contribution in the second term in brace of Eq. (4.3), we take the phenomenological parameter κ as 2.3 [25] in numerical calculations.

The formula of invariant dilepton mass distribution has been derived in [13], which is given by

$$\frac{d\Gamma(B \rightarrow X_s \ell^+ \ell^-)}{ds} = \frac{G_F^2 m_b^5}{768 \pi^5} \alpha_{em}^2 |K_{tb} K_{ts}^*|^2 (1-s)^2 \left(1 - \frac{4r}{s}\right)^{1/2} D(s) \tag{4.12}$$

with

$$\begin{aligned}
D(s) &= 4|C_7^{eff}|^2 \left(1 + \frac{2r}{s}\right) \left(1 + \frac{2}{s}\right) + |C_9^{eff}|^2 \left(1 + \frac{2r}{s}\right) (1+2s) + |C_{10}|^2 \left(1 - 8r + 2s + \frac{2r}{s}\right) \\
&\quad + 12 \text{Re}(C_7^{eff} C_9^{eff*}) \left(1 + \frac{2r}{s}\right) + \frac{3}{2} |C_{Q_1}|^2 (s - 4r) + \frac{3}{2} |C_{Q_2}|^2 s + 6 \text{Re}(C_{10} C_{Q_2}^*) r^{1/2} \tag{4.13}
\end{aligned}$$

where $r = m_\ell^2/m_b^2$. To get rid of large uncertainties due to m_b^5 and CKM elements in Eq. (4.12), we normalized the decay rate to the semileptonic decay rate

$$\Gamma(B \rightarrow X_c \ell \nu) = \frac{G_F^2 m_b^5}{192\pi} |K_{cb}|^2 f\left(\frac{m_c}{m_b}\right) k\left(\frac{m_c}{m_b}\right). \quad (4.14)$$

Here $f(x) = 1 - 8x^2 + 8x^6 - x^8 - 24x^4 \ln x$ is the phase-space factor and $k(x)$ is a sizable next-to-leading QCD correction to the semileptonic decay [26].

The angular information and the forward-backward (FB) asymmetry are also sensitive to the details of the new physics. Defining the forward-backward asymmetry as

$$A_{FB}(s) = \frac{\int_0^1 d \cos \theta (d^2\Gamma/dsd \cos \theta) - \int_{-1}^0 d \cos \theta (d^2\Gamma/dsd \cos \theta)}{\int_0^1 d \cos \theta (d^2\Gamma/dsd \cos \theta) + \int_{-1}^0 d \cos \theta (d^2\Gamma/dsd \cos \theta)}, \quad (4.15)$$

where θ is the angle between the momentum of B-meson and ℓ^+ in the center of mass frame of the dilepton, we obtain

$$A_{FB} = \frac{6(1 - 4r/s)^{1/2}}{D(s)} \text{Re} \left[2C_7^{eff} C_{10}^* + C_9^{eff} C_{10}^* s + 2C_7^{eff} C_{Q_2}^* r^{1/2} + C_9^{eff} C_{Q_1}^* r^{1/2} \right]. \quad (4.16)$$

B. Exclusive decay $B_s \rightarrow \ell^+ \ell^- \gamma$

Now let us turn to the rare radiative decay $B_s \rightarrow \ell^+ \ell^- \gamma$. The exclusive decay can be obtained from the inclusive decay $b \rightarrow s \ell^+ \ell^- \gamma$, and further, from $b \rightarrow s \ell^+ \ell^-$. To achieve this, it is necessary to attach photon to any charged internal and external lines in the Feynman diagrams of $b \rightarrow s \ell^+ \ell^-$. As pointed out in Ref. [3], contributions coming from the attachment of photon to any charged internal line are strongly suppressed and we can neglect them safely. However, since the mass of ℓ -lepton is not much smaller than that of B_s -meson, in $B_s \rightarrow \ell^+ \ell^- \gamma$ decay, the contributions of the diagrams with photon radiating from final leptons are comparable with those from initial quarks. When a photon is attached to the initial quark lines, the corresponding matrix element for the $B \rightarrow \ell^+ \ell^- \gamma$ decay can be written as

$$\begin{aligned} \mathcal{M}_1 = \frac{\alpha_{em}^{3/2} G_F}{\sqrt{2}\pi} K_{tb} K_{ts}^* \{ & [A \varepsilon_{\mu\alpha\beta\sigma} \epsilon_\alpha^* p_\beta q_\sigma + iB(\epsilon_\mu^*(pq) - (\epsilon^* p)q_\mu)] \bar{\ell} \gamma_\mu \ell \\ & + [C \varepsilon_{\mu\alpha\beta\sigma} \epsilon_\alpha^* p_\beta q_\sigma + iD(\epsilon_\mu^*(pq) - (\epsilon^* p)q_\mu)] \bar{\ell} \gamma_\mu \gamma_5 \ell \}, \end{aligned} \quad (4.17)$$

where

$$\begin{aligned} A &= \frac{1}{m_{B_s}^2} \left[C_9^{eff} G_1(p^2) - 2C_7^{eff} \frac{m_b}{p^2} G_2(p^2) \right], \\ B &= \frac{1}{m_{B_s}^2} \left[C_9^{eff} F_1(p^2) - 2C_7^{eff} \frac{m_b}{p^2} F_2(p^2) \right] \\ C &= \frac{C_{10}}{m_{B_s}^2} G_1(p^2), \\ D &= \frac{C_{10}}{m_{B_s}^2} F_1(p^2). \end{aligned} \quad (4.18)$$

In obtaining Eq. (4.17) we have used

$$\langle \gamma | \bar{s} \gamma_\mu (1 \pm \gamma_5) | B_s \rangle = \frac{e}{m_{B_s}^2} \left\{ \varepsilon_{\mu\alpha\beta\sigma} \epsilon_\alpha^* p_\beta q_\sigma G_1(p^2) \mp i [(\epsilon_\mu^*(pq) - (\epsilon^* p)q_\mu)] F_1(p^2) \right\}, \quad (4.19)$$

$$\langle \gamma | \bar{s} i \sigma_{\mu\nu} p_\nu (1 \pm \gamma_5) b | B_s \rangle = \frac{e}{m_{B_s}^2} \left\{ \varepsilon_{\mu\alpha\beta\sigma} \epsilon_\alpha^* p_\beta q_\sigma G_2(p^2) \pm i [(\epsilon_\mu^*(pq) - (\epsilon^* p)q_\mu)] F_2(p^2) \right\}, \quad (4.20)$$

and

$$\langle \gamma | \bar{s} (1 \pm \gamma_5) | B_s \rangle = 0. \quad (4.21)$$

Here ϵ_μ and q_μ are the four vector polarization and momentum of photon, respectively; G_i , F_i are form factors [27,28]. Eq. (4.21) can be obtained by multiplying p_μ in both sides of Eq. (4.20) and using the equations of motion. From Eq. (4.21) one can see that the neutral scalars do not contribute to the matrix element \mathcal{M}_1 .

When a photon is radiated from the final ℓ -leptons, the situation is different. Using the expressions

$$\begin{aligned}\langle 0|\bar{s}b|B_s\rangle &= 0, \\ \langle 0|\bar{s}\sigma_{\mu\nu}(1+\gamma_5)b|B_s\rangle &= 0, \\ \langle 0|\bar{s}\gamma_\mu\gamma_5|B_s\rangle &= -if_{B_s}P_{B_s\mu}\end{aligned}\quad (4.22)$$

and the conservation of the vector current, one finds that only the operators $\mathcal{Q}_{1,2}$ and \mathcal{O}_9 give contribution to this Bremsstrahlung part. The corresponding matrix is given by [4]

$$\begin{aligned}\mathcal{M}_2 &= \frac{\alpha_{em}^{3/2}G_F}{\sqrt{2\pi}}K_{tb}K_{ts}^*i2m_\ell f_{B_s}\left\{(C_{10}+\frac{m_{B_s}^2}{2m_\ell m_b}C_{Q_2})\bar{\ell}\left[\frac{\not{\epsilon}\not{P}_{B_s}}{2p_1q}-\frac{\not{P}_{B_s}\not{\epsilon}}{2p_2q}\right]\gamma_5\ell\right. \\ &\quad \left.+\frac{m_{B_s}^2}{2m_\ell m_b}C_{Q_1}\left[2m_\ell\left(\frac{1}{2p_1q}+\frac{1}{2p_2q}\right)\bar{\ell}\not{\epsilon}\ell+\bar{\ell}\left(\frac{\not{\epsilon}\not{P}_{B_s}}{2p_1q}-\frac{\not{P}_{B_s}\not{\epsilon}}{2p_2q}\right)\ell\right]\right\}.\end{aligned}\quad (4.23)$$

Here P_{B_s} , f_{B_s} are the momentum and the decay constant of the B_s meson, p_1 , p_2 are momenta of the final ℓ -leptons.

Finally, the total matrix element for the $B_s \rightarrow \ell^+\ell^-\gamma$ decay is obtained as a sum of the \mathcal{M}_1 and \mathcal{M}_2 . After summing over the spins of the ℓ -leptons and polarization of the photon, we get the square of the matrix element as

$$|\mathcal{M}|^2 = |\mathcal{M}_1|^2 + |\mathcal{M}_2|^2 + 2Re(\mathcal{M}_1\mathcal{M}_2^*) \quad (4.24)$$

with

$$\begin{aligned}|\mathcal{M}_1|^2 &= 4\left|\frac{\alpha_{em}^{3/2}G_F}{\sqrt{2\pi}}K_{tb}K_{ts}^*\right|^2\left\{[|A|^2+|B|^2]\left[p^2((p_1q)^2+(p_2q)^2)+2m_\ell^2(pq)^2\right]\right. \\ &\quad \left.+[|C|^2+|D|^2]\left[p^2((p_1q)^2+(p_2q)^2)-2m_\ell^2(pq)^2\right]\right. \\ &\quad \left.+2Re(B^*C+A^*D)p^2((p_1q)^2-(p_2q)^2)\right\},\end{aligned}\quad (4.25)$$

$$\begin{aligned}2Re(\mathcal{M}_1\mathcal{M}_2^*) &= -16\left|\frac{\alpha_{em}^{3/2}G_F}{\sqrt{2\pi}}K_{tb}K_{ts}^*\right|^2m_\ell^2f_{B_s}(pq)^2\left\{|C_{10}+\frac{m_{B_s}^2}{2m_\ell m_b}C_{Q_2}|\left[Re(A)\frac{(p_1q+p_2q)}{(p_1q)(p_2q)}\right.\right. \\ &\quad \left.\left.-Re(D)\frac{(p_1q-p_2q)}{(p_1q)(p_2q)}\right]+Re(B)\left|\frac{m_{B_s}^2C_{Q_1}}{2m_\ell m_b}\right|\left[\frac{3m_{B_s}^2+2m_\ell^2-5(pq)}{(p_1q)(p_2q)}-\frac{2p^2}{(pq)^2}\right]\right. \\ &\quad \left.+Re(C)\left|\frac{m_{B_s}^2C_{Q_1}}{2m_\ell m_b}\right|\left[\frac{(p_1q-p_2q)}{(p_1q)(p_2q)}\left(1+\frac{2p^2}{(pq)^2}\right)\right]\right\},\end{aligned}\quad (4.26)$$

$$\begin{aligned}|\mathcal{M}_2|^2 &= -8\left|\frac{\alpha_{em}^{3/2}G_F}{\sqrt{2\pi}}K_{tb}K_{ts}^*\right|^2m_\ell^2f_{B_s}^2\left\{|C_{10}+\frac{m_{B_s}^2}{2m_\ell m_b}C_{Q_2}|^2\left[\frac{m_\ell^2m_{B_s}^2(pq)^2}{(p_1q)^2(p_2q)^2}-\frac{m_{B_s}^2p^2+2(pq)^2}{(p_q)(p_2q)}\right]\right. \\ &\quad \left.-\left|\frac{m_{B_s}^2C_{Q_1}}{2m_\ell m_b}\right|^2\left[\frac{m_\ell^2(m_{B_s}^2-4m_\ell^2)(pq)^2}{(p_1q)^2(p_2q)^2}-\frac{(m_{B_s}^2-4m_\ell^2)p^2+2(pq)^2}{(p_1q)(p_2q)}\right]\right\}.\end{aligned}\quad (4.27)$$

It is obvious that the quantity $|\mathcal{M}|^2$ depends only on the scalar products of the momenta of the external particles. In this paper, we follow Ref. [3] and consider the photon in $B_s \rightarrow \ell^+\ell^-\gamma$ as a hard photon and impose a cut on the photon energy E_γ ², which correspond to the radiated photon can be detected in the experiments. This cut requires $E_\gamma \geq \delta m_{B_s}/2$ with $\delta = 0.02$.

After integrating over the phase space and the lepton energy E_1 , we express the decay rate as

²When photon is soft, both processes of $B_s \rightarrow \ell^+\ell^-\gamma$ and $B_s \rightarrow \ell^+\ell^-$ should be considered together, and in this case, the infrared singular terms in $|\mathcal{M}_2|^2$ can be canceled exactly by the $O(\alpha_{em})$ virtual correction in $B_s \rightarrow \ell^+\ell^-$ [3].

$$\begin{aligned}
\Gamma = & \left| \frac{\alpha_{em}^{3/2} G_F}{2\sqrt{2}\pi} K_{tb} K_{ts}^* \right|^2 \frac{m_{B_s}^5}{(2\pi)^3} \left\{ \frac{m_{B_s}^2}{12} \int_{4\hat{r}}^{1-\delta} (1-\hat{s})^3 d\hat{s} \sqrt{1-\frac{4\hat{r}}{\hat{s}}} [(|A|^2 + |B|^2) (\hat{s} + 2\hat{r}) \right. \\
& + (|C|^2 + |D|^2) (\hat{s} - 4\hat{r})] - 2f_{B_s} |C_{10} + \frac{m_{B_s}^2 C_{Q_2}}{2m_\ell m_b} | \hat{r} \int_{4\hat{r}}^{1-\delta} (1-\hat{s})^2 d\hat{s} \text{Re}(A) \ln \hat{z} \\
& - 2f_{B_s} \left| \frac{m_{B_s}^2 C_{Q_1}}{2m_\ell m_b} \right| \hat{r} \int_{4\hat{r}}^{1-\delta} (1-\hat{s}) d\hat{s} \text{Re}(B) \left[(1+4\hat{r}+5\hat{s}) \ln \hat{z} + \hat{s} \sqrt{1-\frac{4\hat{r}}{\hat{s}}} \right] \\
& - \frac{4f_{B_s}^2}{m_{B_s}^2} |C_{10} + \frac{m_{B_s}^2 C_{Q_2}}{2m_\ell m_b} |^2 \hat{r} \int_{4\hat{r}}^{1-\delta} d\hat{s} \left[\left(1 + \hat{s} + \frac{4\hat{r}-2}{1-\hat{s}}\right) \ln \hat{z} + \frac{2\hat{s}}{1-\hat{s}} \sqrt{1-\frac{4\hat{r}}{\hat{s}}} \right] \\
& \left. + f_{B_s}^2 \left| \frac{C_{Q_1}}{m_b} \right|^2 \int_{4\hat{r}}^{1-\delta} d\hat{s} \left[\left(1 - 8\hat{r} + \hat{s} - \frac{2-10\hat{r}+8\hat{r}^2}{1-\hat{s}}\right) \ln \hat{z} + \frac{2(1-4\hat{r})\hat{s}}{1-\hat{s}} \sqrt{1-\frac{4\hat{r}}{\hat{s}}} \right] \right\}, \quad (4.28)
\end{aligned}$$

where $\hat{s} = p^2/m_{B_s}^2$, $\hat{r} = m_\ell^2/m_{B_s}^2$, $\hat{z} \equiv Z(\hat{r}, \hat{s})$ takes the form given in Eq. (4.11).

V. EXPERIMENTAL CONSTRAINTS ON THE RELEVANT SUSY PARAMETERS

Before scanning the relevant parameter space of MSSM, we assume (i) the masses of the particles are restricted to the sub-TeV regime and larger than the lower experimental bounds [21]; (ii) A-parameters are smaller than $3M_{\tilde{Q}}$ [29]; (iii) Except for the third generation squarks, all sfermions are degenerate and have masses of $\sim 1\text{TeV}$; (iv) The GUT mass relation $M_1 \approx M_2/2$ for gauginos is used; (v) Only small flavor violation $\epsilon_i < 0.1$ is allowed. We also take into account the well-known large radiative corrections to neutral Higgs masses [30]. With above assumptions and gluino mass fixed as its lower experimental bound 190 GeV [21], the relevant parameter space is determined by nine input parameters: $M_{\tilde{Q}}, M_{\tilde{t}_R}, M_{\tilde{b}_R}, \mu, \tan\beta, A_t, A_b, M_2$ and m_A . In addition, we consider the following the experimental constraints in our scan:

(1) The recently reported value of muon $g-2$ [19] shows a 2.6 standard deviation from its SM prediction. The SUSY explanation of this deviation requires (i) $\mu > 0$ and (ii) large $\tan\beta$. In our calculation we assume $20 \leq \tan\beta \leq 90$ and at least one of the charginos or neutralinos must be lighter than 500 GeV [18].

(2) Non-observation of any supersymmetric signals at CERN e^+e^- collider LEP-II and the Fermilab Tevatron imposes lower bounds as

$$\begin{aligned}
m_{H^\pm} &\geq 78.6\text{ GeV} & m_{h^0} &\geq 88.3\text{ GeV}, & m_{\tilde{\chi}_1^\pm} &\geq 67.7\text{ GeV}, \\
m_{\tilde{\chi}_1^0} &\geq 42.0\text{ GeV} & m_{\tilde{t}_1} &\geq 86.4\text{ GeV}, & m_{\tilde{b}_1} &\geq 75.0\text{ GeV}.
\end{aligned} \quad (5.1)$$

(3) The latest measurement of the inclusive branching ratio from CLEO and BELLE [2] gives world average value

$$2.44 \times 10^{-4} < Br(B \rightarrow X_s \gamma) < 4.02 \times 10^{-4} \quad (95\% \text{ C. L.}), \quad (5.2)$$

which is specially useful to constrain extensions of the SM. Previous studies used leading-order (LO) SM result to limit the MSSM parameter space. Instead of LO calculation [12,31], the branching ratio of $B(B \rightarrow X_s \gamma)$ has been estimated at next-leading-order (NLO) level in the SM [24] with about 22.5% increase of its central value and theoretical error less than 10%. In this paper, we use the SM result computed at NLO level whereas the additional supersymmetric contributions at LO level. We do not use the available NLO matching conditions for the supersymmetric particles since they are computed under the specific assumptions about the sparticle spectrum, not necessarily satisfied in the criteria, and moreover, they are not valid for large values of $\tan\beta$ [8]. Since the Wilson coefficient C_8 accounts for only 3% of the standard model $b \rightarrow s\gamma$ amplitude, it is therefore not expected to be significantly more important in the MSSM. In this case, Eq. (5.2) implies the constraints on the ratio $R_7 = C_{7,MSSM}^{0,eff}/C_{7,SM}^{0,eff}$

$$0.83 \leq R_7 \leq 1.13, \quad \text{or} \quad -1.24 \leq R_7 \leq -0.94. \quad (5.3)$$

(4) The stringent bounds on the magnitude of the short distance coefficients come from the Collider Detector at Fermilab (CDF) [21]

$$\begin{aligned}
Br(B^+ \rightarrow K^+ \ell^+ \ell^-) &< (60, 5.2) \times 10^{-6} \quad (90\% \text{ C.L.}), \\
Br(B^0 \rightarrow K^{*0} \ell^+ \ell^-) &< (290, 4.0) \times 10^{-6} \quad (90\% \text{ C.L.}), \\
Br(B_s \rightarrow \ell^+ \ell^-) &< (5.4, 2.0) \times 10^{-6} \quad (95\% \text{ C.L.})
\end{aligned} \quad (5.4)$$

for $\ell = e, \mu$.

VI. NUMERICAL RESULTS AND DISCUSSIONS

We perform a complete scan over the nine-dimensional parameter space of the MSSM. For reference, we present our SM predictions

$$Br(B \rightarrow X_s \ell^+ \ell^-) = (11.8, 9.87, 2.94) \times 10^{-6}, \quad (6.1)$$

$$Br(B_s \rightarrow \ell^+ \ell^- \gamma) = (2.50, 2.62, 5.49) \times 10^{-8} \quad (6.2)$$

for $\ell = e, \mu, \tau$. These values are obtained by taking the QCD coupling constant $\alpha_s(m_b) = 0.218$, the masses, decay widths and branching ratios of J/Ψ family in Ref. [21], the normalized factor $Br(B \rightarrow X_c \ell \nu) = 10.2\%$ and the form-factors [28]

$$\begin{aligned} G_1(p^2) &= \frac{1 \text{ GeV}}{(1 - p^2/5.6^2)^2}, & G_2(p^2) &= \frac{3.74 \text{ GeV}}{(1 - p^2/40.5)^2}, \\ F_1(p^2) &= \frac{0.8 \text{ GeV}}{(1 - p^2/6.5^2)^2}, & F_2(p^2) &= \frac{0.68 \text{ GeV}}{(1 - p^2/30)^2}. \end{aligned} \quad (6.3)$$

as well as the fixed input parameters [21] listed in Table I in the numerical calculations.

Table I. The value of the input parameters used in the numerical calculations (mass and decay constant in unit GeV).

m_t	m_c	m_b	m_τ	m_{B_s}	m_W
176	1.4	4.8	1.78	5.26	80.45
f_{B_s}	$ K_{tb} K_{ts}^* $	$ K_{tb} K_{ts}^* / K_{cb} ^2$	α_{em}^{-1}	$\tau(B_s)$	$\sin^2 \theta_W$
0.21	0.045	0.95	137	$1.64 \times 10^{-12} s$	0.233

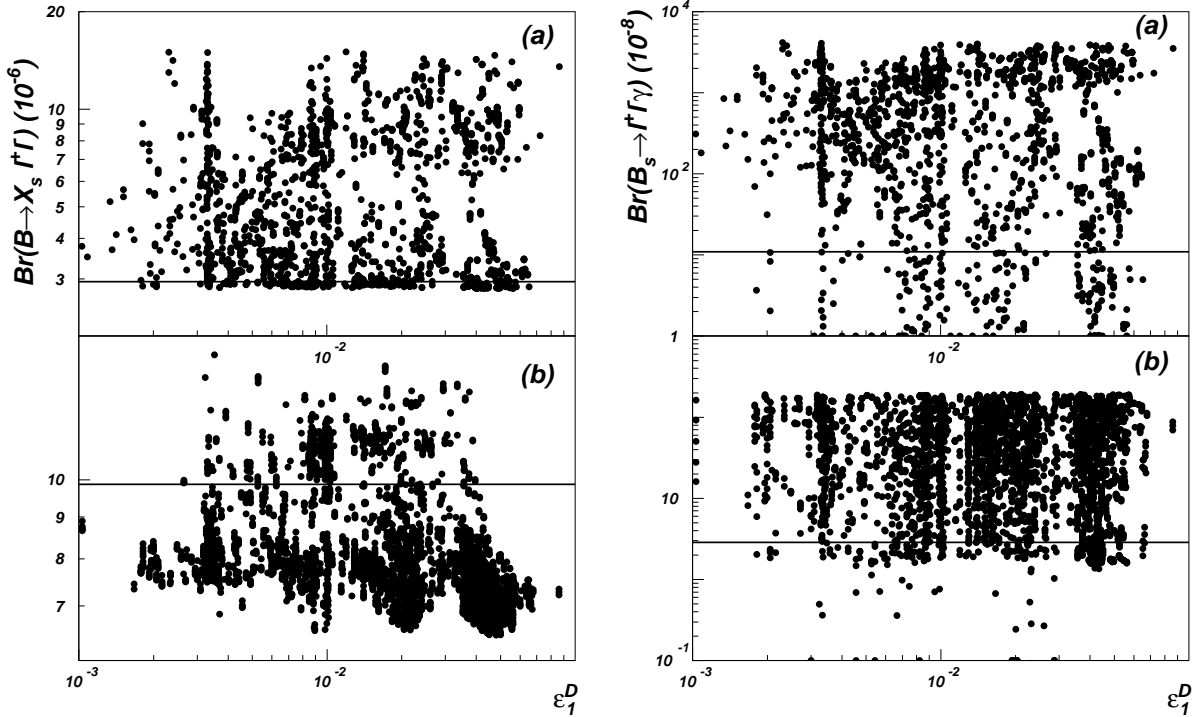


FIG. 4. The parameter space scatter plot of $Br(B \rightarrow X_s \ell^+ \ell^-)$ (left) and $Br(B_s \rightarrow \ell^+ \ell^- \gamma)$ (right) vs ϵ_1 for $\ell = \tau$ in (a) and for $\ell = \mu$ in (b). The solid lines stand for the SM predictions

The results shown in Fig. 4 indicates that in some part of parameter space, the enhancement factors R of the branching ratios can be 5 for the inclusive decay $B \rightarrow X_s \tau^+ \tau^-$ and a couple of orders of magnitude over the standard model predictions for the exclusive decay $B_s \rightarrow \tau^+ \tau^- \gamma$. This is quite different from the previous studies [11]. As illustrative examples, the branching ratios for ditau final state as functions of the gluino mass are plotted in Fig. 5. The effects drop with the increase of gluino mass, showing the decoupling property of the MSSM. Table 2 shows the case in which both enhancement factors reach their maximum values and the corresponding SUSY parameters. A comparison of the enhancement factors with and without the NCL effects is also presented.

Table II. The maximum enhancement factors and their corresponding SUSY parameters (mass in unit GeV).

$R_{max}(B \rightarrow X_s \tau \tau)$		$R_{max}(B_s \rightarrow \tau \tau \gamma)$	
With NCL	without NCL	With NCL	without NCL
4.34	0.99	327.0	0.75
$\tan \beta = 40$	$m_A = 453$	$m_{\tilde{t}_1} = 143$	$m_{\tilde{b}_1} = 92$

We have the following comments on the results:

(1) The constraint on $B_s \rightarrow \ell^+ \ell^-$ is of special useful to limit the effects of the scalars and pseudo-scalars. However, since no helicity suppression compared with C_{10} (see Eq. 4.23), the contribution of $C_{Q_{1,2}}$ in $B \rightarrow X_s \tau^+ \tau^-$ and $B_s \rightarrow \ell^+ \ell^- \gamma$ decay is still dominate for large $\tan \beta$.

(2) As helicity suppression, the effects of $C_{Q_{1,2}}$ in $B \rightarrow X_s \tau^+ \tau^-$ are very different from those with other dilepton final states (see Eq. 4.13). The smaller mass of lepton in the final states, the less effect of gluino and the neutralinos. In the inclusive decays with lighter dilepton final states, the dominate contribution comes from the interaction term $2Re(C_7^{eff} C_9^{eff})$ with opposite sign to its SM value. For large $\tan \beta$ region, relative large m_τ make the neutral Higgs with NCL contribute sizably to the inclusive decay.

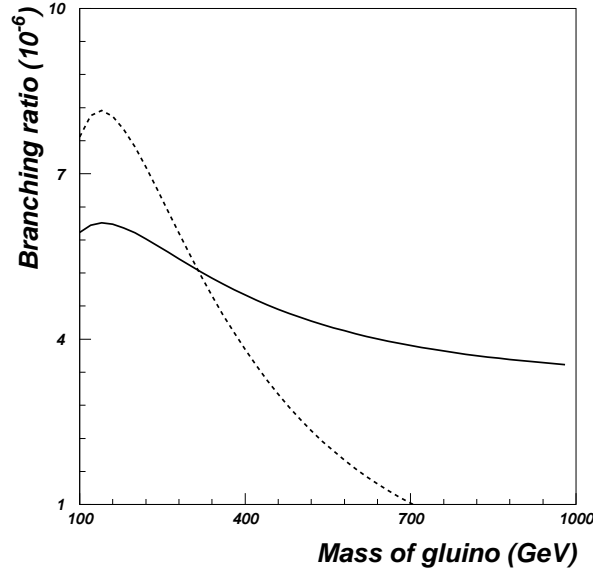


FIG. 5. The branching ratios vs gluino mass with $\tan \beta = 40$, $m_A = 271$ GeV, $m_{\tilde{t}_1} = 320$ GeV, $m_{\tilde{b}_1} = 265$ GeV. The solid and dashed lines correspond to the inclusive and exclusive decays with $\ell = \tau$, respectively.

Some numerical examples in the region of $R_7 > 0$ are presented in Figs. 6-8. Fig. 6 and Fig. 7 show the branching ratios of $B \rightarrow X_s \tau^+ \tau^-$ and $B_s \rightarrow \tau^+ \tau^- \gamma$, respectively. For the specified parameter values in the figures, one sees that the contributions from gluino and neutralinos are dominant. When the mass of the CP-odd Higgs is less than 700 GeV or $\tan \beta > 40$, the branching ratio of $B \rightarrow X_s \tau^+ \tau^-$ can be enhanced by a factor 2, and for $B_s \rightarrow \tau^+ \tau^- \gamma$, by one order over the SM results.

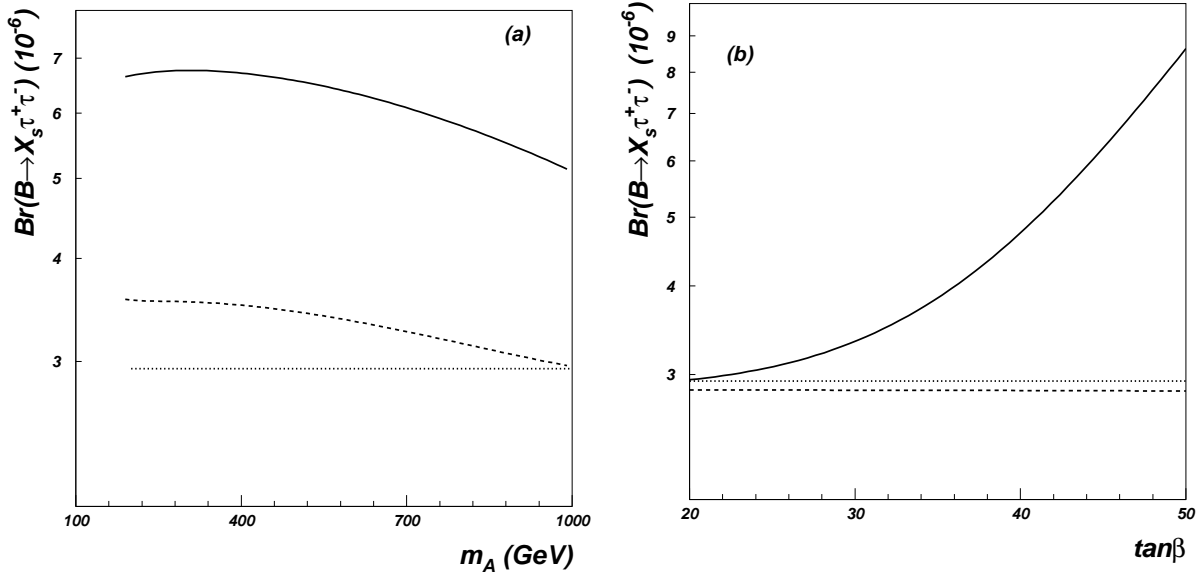


FIG. 6. Branching ratio of $B \rightarrow X_s \tau^+ \tau^-$ versus m_A in (a) and versus $\tan\beta$ in (b). The dotted line stands for the SM prediction, whereas the solid (dashed) one is the MSSM prediction with (without) the contributions of the gluino and neutralinos. The parameter space in (a) is specified as $m_{\tilde{t}} = (179, 304)$ GeV, $m_{\tilde{b}} = (257, 700)$ GeV, $m_{\tilde{\chi}^\pm} = (94, 417)$ GeV, $m_{\tilde{\chi}^0} = (81, 109, 200, 417)$ GeV and $\tan\beta = 20$; In (b), $m_A = 899$ GeV, the masses of the sparticles are dependent on the value of $\tan\beta$.

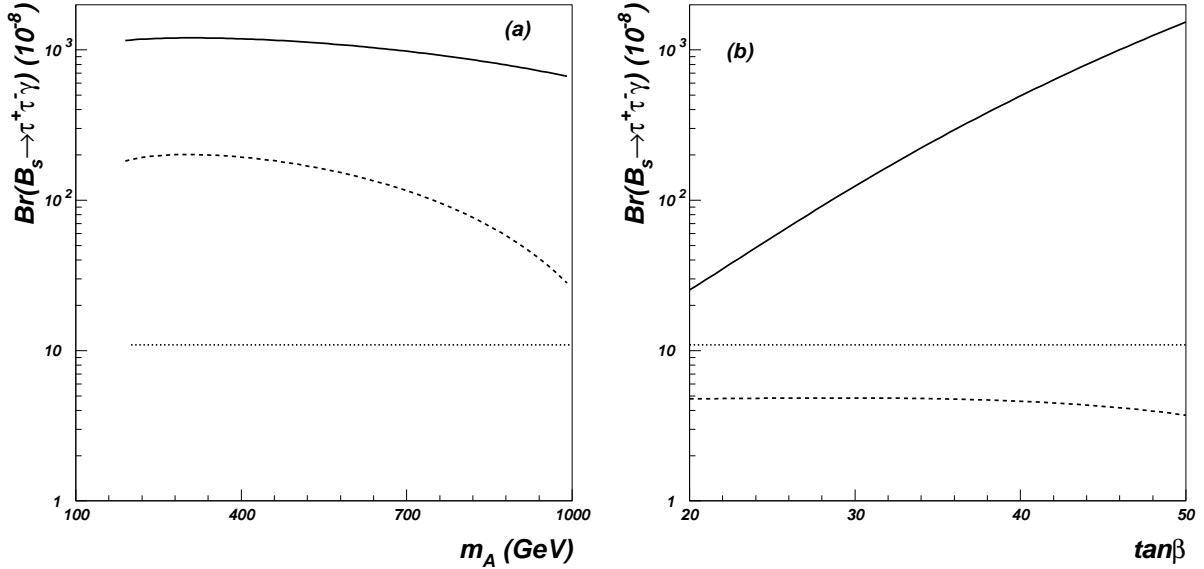


FIG. 7. The same as Fig. 6, but for $B_s \rightarrow \tau^+ \tau^- \gamma$.

The differential branching ratios of $B \rightarrow X_s \tau^+ \tau^-$ and $B_s \rightarrow \tau^+ \tau^- \gamma$ versus the scaled invariant dilepton mass squared are plotted in Fig. 8, while the dependence of the FB asymmetry for $B \rightarrow X_s \tau^+ \tau^-$ on the scaled invariant dilepton mass squared is shown in Fig. 9. The figures show significant differences between the SM and the MSSM predictions, especially in large invariant dilepton mass region.

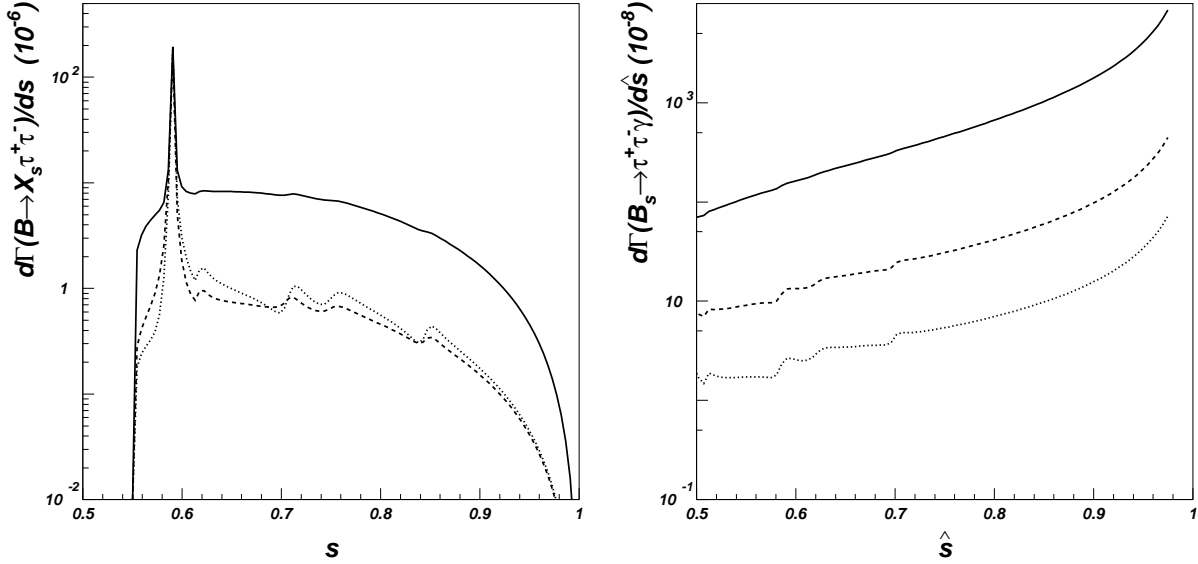


FIG. 8. The same as Fig. 6a, but for the differential branching ratios of $B \rightarrow X_s \tau^+ \tau^-$ and $B_s \rightarrow \tau^+ \tau^- \gamma$ versus the scaled invariant dilepton mass squared with $m_A = 305 \text{ GeV}$.

We should point out that since some common contributions appearing in both the numerator and the denominator cancel out to some extent, the FB asymmetry is a sensitive, relatively model-independent probe of these models. We stress that all these distributions would be useful for fitting the future experimental results in the framework of the MSSM, especially when some deviations from the SM predictions are discovered in future experiments. Different models, such as the MSSM and 2HDM's, may all predict some enhancements, but they may give different behaviors for some distributions.

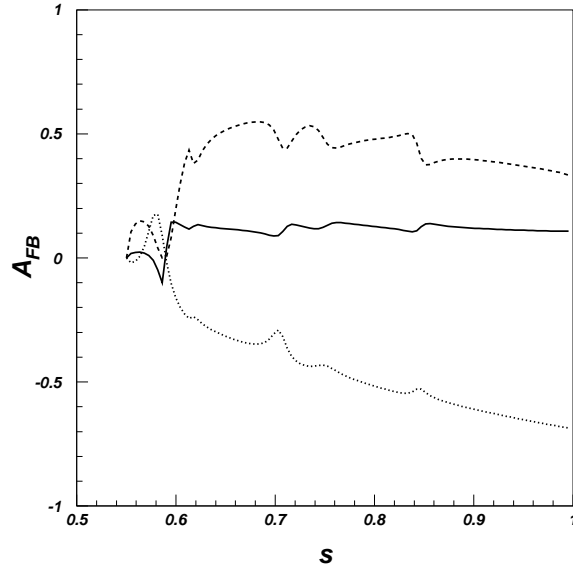


FIG. 9. The same as Fig. 6a, but for the forward-backward asymmetry of $B \rightarrow X_s \tau^+ \tau^-$ versus the scaled invariant dilepton mass squared s with $m_A = 305 \text{ GeV}$.

Although decay modes with the ditau final states are experimentally difficult compared to their di-muonic counterparts, the considered decay modes are more sensitive to new physics. More theoretical studies, such as higher order effects which might also lead to important modifications as in the case of $B \rightarrow X_s \gamma$ [32], and experimental efforts for the decays considered are valuable.

VII. CONCLUSION

In this work we performed a complete one-loop calculation of the inclusive decay $B \rightarrow X_s \ell^+ \ell^-$ and exclusive decay $B_s \rightarrow \ell^+ \ell^- \gamma$ in the MSSM. Various experimental constraints on the relevant SUSY parameters, such as $B \rightarrow X_s \gamma$, $B \rightarrow K^{(*)} \ell^+ \ell^-$, $B_s \rightarrow \ell^+ \ell^-$ and the latest $g_\mu - 2$ experimental measurement, were considered to constrain the parameter space of the MSSM. Our results showed that the contributions from the gluino and neutralino loops, which were neglected in previous studies, might be quite important or even dominant in some part of parameter space. These supersymmetric contributions could significantly enhance the branching ratios over the SM predictions. Also, with these contributions the distributions of the forward-backward asymmetry of $B \rightarrow X_s \tau^+ \tau^-$ and some other distributions could differ significantly from their SM predictions. Up to now the currently running B-factories such as *BaBar* at SLAC [33] and BELLE at KEKB [34] have collected about $3.2 \times 10^7 B\bar{B}$ pair with a luminosity of $(3 \sim 4) \times 10^{33} \text{ cm}^{-2} \text{ s}^{-1}$ [33,34]. And the *BaBar* will take $10^8 B\bar{B}$ pairs in three years while the BELLE $10^7 B\bar{B}$ pairs each year. Since the branching ratios of the inclusive decay $B \rightarrow X_s \tau^+ \tau^-$ and exclusive decay $B_s \rightarrow \tau^+ \tau^- \gamma$ can be enhanced by the SUSY effects with large $\tan\beta$ to reach the level of 10^{-5} , these ditau decays might be observable at the B factories.

ACKNOWLEDGMENT

We would like thank Prof. A. Ali and C.-P. Yuan for useful discussion. This work is supported in part by a grant of Chinese Academy of Science for Outstanding Young Scholars.

APPENDIX

In the Appendix we present the operator basis O_i , Q_i and one-loop integral functions for $b \rightarrow s \ell^+ \ell^-$. The operator basis O_i is the same as the one used for the $b \rightarrow s \ell^+ \ell^-$ in the SM,

$$\begin{aligned}
\mathcal{O}_1 &= (\bar{s}_\alpha \gamma^\mu L c_\beta) (\bar{c}_\beta \gamma^\mu L b_\alpha), \\
\mathcal{O}_2 &= (\bar{s}_\alpha \gamma^\mu L c_\alpha) (\bar{c}_\beta \gamma^\mu L b_\beta), \\
\mathcal{O}_{3,5} &= (\bar{s}_\alpha \gamma^\mu L c_\alpha) \left(\sum_q \bar{q}_\beta \gamma^\mu (L, R) b_\beta \right), \\
\mathcal{O}_{4,6} &= (\bar{s}_\alpha \gamma^\mu L c_\beta) \left(\sum_q \bar{q}_\beta \gamma^\mu (L, R) b_\alpha \right), \\
\mathcal{O}_7 &= \frac{e}{16\pi^2} \bar{s}_\alpha \sigma^{\mu\nu} (m_b R + m_s L) b_\alpha F_{\mu\nu}, \\
\mathcal{O}_8 &= \frac{g_s}{16\pi^2} \bar{s}_\alpha \sigma^{\mu\nu} (m_b R + m_s L) t_{\alpha\beta} b_\beta G_{\mu\nu}^\alpha, \\
\mathcal{O}_9 &= \frac{e}{16\pi^2} (\bar{s}_\alpha \gamma^\mu L b_\alpha) (\bar{\ell} \gamma_\mu \ell), \\
\mathcal{O}_{10} &= \frac{e}{16\pi^2} (\bar{s}_\alpha \gamma^\mu L b_\alpha) (\bar{\ell} \gamma_\mu \gamma_5 \ell),
\end{aligned} \tag{7.1}$$

where the chiral structure is specified by the projectors $L, R = (1 \mp \gamma_5)/2$, while α and β are color indices. $F_{\mu\nu}$ and $G_{\mu\nu}^\alpha$ denote the QED and QCD field strength tensors, respectively. $t_{\alpha\beta}$ are the color triplet generators, g and g_s stand for the electromagnetic and strong coupling constants.

Operators Q_i come from exchanging the neutral Higgs bosons in MSSM and are defined by [13]

$$\begin{aligned}
\mathcal{Q}_1 &= \frac{g^2}{16\pi^2} (\bar{s}_\alpha R b_\alpha) (\bar{\ell} \ell), \\
\mathcal{Q}_2 &= \frac{g^2}{16\pi^2} (\bar{s}_\alpha R b_\alpha) (\bar{\ell} \gamma_5 \ell), \\
\mathcal{Q}_{3,4} &= \frac{g^2}{16\pi^2} (\bar{s}_\alpha R b_\alpha) \left(\sum_q \bar{s}_\beta (R, L) b_\beta \right),
\end{aligned}$$

$$\begin{aligned}
\mathcal{Q}_{5,6} &= \frac{g^2}{16\pi^2} (\bar{s}_\alpha R b_\beta) \left(\sum_q \bar{s}_\beta(R, L) b_\alpha \right), \\
\mathcal{Q}_{7,8} &= \frac{g^2}{16\pi^2} \bar{s}_\alpha \sigma^{\mu\nu} R b_\alpha \left(\sum_q \bar{s}_\beta(R, L) b_\beta \right), \\
\mathcal{Q}_{9,10} &= \frac{g^2}{16\pi^2} \bar{s}_\alpha \sigma^{\mu\nu} R b_\beta \left(\sum_q \bar{s}_\beta(R, L) b_\alpha \right).
\end{aligned} \tag{7.2}$$

The one-loop integral functions which appear within the MSSM matching conditions are given by

$$\begin{aligned}
P_1(x) &= \frac{1}{x-1} \ln x, \\
P_2(x, y) &= \frac{1}{(x-y)} \left[\frac{x^2}{x-1} \ln x - \frac{y^2}{y-1} \ln y \right], \\
P_3(x, y) &= \frac{1}{(x-y)} \left[\frac{x}{x-1} \ln x - \frac{y}{y-1} \ln y \right], \\
P_4(x, y, z) &= \left[\frac{x}{(x-1)(x-y)(x-z)} \ln x + (x \leftrightarrow y) + (x \leftrightarrow z) \right].
\end{aligned} \tag{7.3}$$

- [1] R. Ammar, *et al.*, CLEO Collaboration, Phys. Rev. Lett. **71** (1993) 674; M. S. Alam *et al.*, CLEO Collaboration, Phys. Rev. Lett. **74**(1995) 2885.
- [2] S. Glem, *et al.*, CLEO Collaboration, hep-ex/0104045; K. Abe, *et al.*, BELLE Collaboration Phys. Lett. **B511**, 151, (2001).
- [3] T. Goto, Y. Okada, Y. Shinizu and M. Tanada, Phys. Rev. **D55**, 4273 (1997); T. M. Aliev, A. Özpineci and M. Savci, Phys. Rev. **D55**, 7059 (1997); T. M. Aliev, N. K. Pak and M. Savci, Phys. Lett. **B424**, 175 (1998).
- [4] E. O. Iltan and G. Turan, Phys. Rev. D **61**, 034010 (2000).
- [5] Z. Xiong and J. M. Yang, Nucl. Phys. **B602** 289 (2001); Y. Su, Phys. Rev. D **56**, 335 (1997).
- [6] M. Misiak, Nucl. Phys. **B393**, 23 (1993); A. F. Falk, M. Luke and M. Savage, Phys. Rev. **D49**, 3367 (1994); Z. Ligeti and M. B. Wise, Phys. Rev. **D53**, 4937 (1996); F. Krüger and L. M. Sehgal, Phys. Lett. **B380**, 199 (1996); A. Ali, G. Hiller, L. T. Handoso and T. Morozumi, Phys. Rev. **D55**, 4105 (1997); J-W. Chen, G. Rupak and J. Savage, Phys. Lett. **B410**, 285 (1997); G. Buchalla, G. Isidori and S. J. Rey, Nucl. Phys. **B511**, 594 (1998); G. Buchalla, G. Isidori, Nucl. Phys. **B525**, 333 (1998).
- [7] C. Bobeth, M. Misiak and J. Urban, Nucl. Phys. **B574**, 291 (2000); H. H. Asatryan, H. M. Asatrian, C. Greub and M. Walker, Phys. Lett. **B507**, 162 (2001).
- [8] P. H. Chankowski and L. Slawianowska, Phys. Rev. D **63**, 054012 (2001);
- [9] P. Cho, M. Misiak and D. Wyler, Phys. Rev. **D54**, 3329 (1997); Y. Grossman, Z. Ligeti, and E. Nardi, Phys. Rev. **D55**, 2768 (1997); J. L. Hewett and J. D. Wells, Phys. Rev. **D55**, 5549 (1997).
- [10] S. Bertolini, F. Borzumati, A. Masiero, and G. Ridolfi, Nucl. Phys. **B353**, 591 (1991); A. J. Buras and M. Münz, Phys. Rev. D **52**, 186 (1995); M. Ciuchini, G. Degrassi, P. Gambino, and G. F. Giudice, Nucl. Phys. **B527**, 21 (1998); **B534,3** (1998).
- [11] C. S. Huang, W. Liao, Q. S. Yan and S.-H. Zhu, Phys. Rev. **D59**, 011701 (1999); C. S. Huang and S.-H. Zhu, Phys. Rev. **D61**, 015011 (2000); C. S. Huang, W. Liao, Q. S. Yan and S.-H. Zhu, Phys. Rev. **D63**, 114021 (2001); C. S. Huang, W. Liao, Q. S. Yan and S.-H. Zhu, hep-ph/0110147; S. R. Choudury, N. Gaur, Phys. Lett. **B451**, 86 (1999).
- [12] B. Grinstein, R. Springer, and M. B. Wise, Phys. Lett. **B202**, 138 (1988); Nucl. Phys. **B339**, 269 (1990).
- [13] Y. B. Dai, C. S. Huang and H. W. Huang, Phys. Lett. **B390**, 257 (1997);
- [14] J. L. Hewett, Phys. Rev. **D53**, 4964 (1996).
- [15] H. E. Logan and U. Nierste, Nucl. Phys. **B586**, 39 (2000); C. Bobeth, T. Ewerth, F. Krüger and J. Urban, hep-ph/0104284; G. Erkol and G. Turan, hep-ph/0110017; G. K. Yeghiyan, hep-ph/0108151.
- [16] H. E. Haber and G. L. Kane, Phys. Reports. **117**, 75 (1985).
- [17] See, *e. g.*, the L3 collaboration, Phys. Lett. **B503**, 21 (2001)
- [18] L. Everett, C. L. Kane, S. Rigolin and L.-T. Wang, Phys. Rev. Lett. **86**, 3484 (2001), J. L. Feng and K. T. Matchev, Phys. Rev. Lett. **86**, 3480 (2001).

- [19] H. N Brown, *et al.*, Mu $g-2$ Collaboration, Phys. Rev. Lett.**86**, 2227 (2001).
- [20] See, e.g., M. J. Duncan, Nucl. Phys. B **221**, 285 (1983).
- [21] Particle Physics Group. Eur. Phys. J. C, **15**, 274 (2000).
- [22] K. I. Hikasa and M. Kobayashi, Phys. Rev. D**36**, 724 (1987); J. M. Yang and C. S. Li, Phys. Rev. D**49**, 3412 (1994).
- [23] E. Lunghi, A. Masiero, I. Scimemi, L. Silvestrini, Nucl. Phys. B**568**, 120 (2000).
- [24] K. Chetykin, M. Misiak, and M. Münz, Phys. Lett. B **400**, 206 (1997); C. Greub and T. Hurth, Phys. Rev. D **56**, 2934 (1997). F. M. Borzumati and C. Greub, Phys. Rev. D**58**, 074004 (1998).
- [25] A. Ali and C. Greub, Z. Phys. C **49**, 431 (1991); Phys. Lett. B **259**, 182 (1991); **361**, 146 (1995); A. Ali, B. Ball, L. T. Handoko and G. Hiller, Phys. ReV. D**61**, 074024 (2000).
- [26] N. Cabibbo and L. Maiani, Phys. Lett. B**79**, 109 (1978); Y. Nir, Phys. Lett. B**221**, 184 (1989).
- [27] G. Buchalla and A. J. Buras, Nucl. Phys. B**400**, 225 (1993); D. Du, C. Liu and D. Zhang, Phys. Lett. B **317**, 179 (1993).
- [28] G. Eilam, I. Halperin and R. R. Mendel, Phys. Lett. B**361**, 137 (1995).
- [29] H. E. Haber, Lectures Given at Theoretical Advanced Study Institute, 1992.
- [30] A. Djouadi, J. Kalinowski and M. Spira, Comput. Phys. Commun.**108**, 56 (1996).
- [31] M. Ciuchini, E. Franco, G. Martinelli, L. Reina, and L. Siliverstrini, Phys. Lett. B **316**, 127 (1993); M. Ciuchini, E. Franco, G. Martinelli, L. Reina Phys. Lett. B **301**, 263 (1993), Nucl. Phys. B **415**, 403 (1994); M. Ciuchini, E. Franco, L. Reina, and L. Siliverstrini, Phys. Lett. B **421**, 41 (1994);
- [32] G. Degross et al, JHEP**0012**, 009 (2000); M. Carena et al., Phys. Lett. B**99**, 14 (2001).
- [33] *BaBar* Collaboration, B. Aubert *et al.*, hep-ex/0105044; Phys. Rev. Lett.**86**, 2515 (2001).
- [34] Belle Collaboration, A. Abashian *et al.*, Phys. Rev. Lett.**87**, 091801 (2001).